Journal of Electrochemistry

Volume 26
Issue 5 *Memorial Special Issue for Professor Chuansin Cha*

2020-10-28

A Model for the Anodic Carbonization of Alkaline Polymer Electrolyte Fuel Cells

Qi-hao LI

Ying-ming WANG

Hua-long MA

Li XIAO

Gong-wei WANG

Jun-tao LU
College of Chemistry and Molecular Sciences, Hubei Key Lab of Electrochemical Power Sources,Wuhan University, Wuhan 430072, China;, jtlu@whu.edu.cn

Lin ZHUANG
College of Chemistry and Molecular Sciences, Hubei Key Lab of Electrochemical Power Sources,Wuhan University, Wuhan 430072, China;, lzhuang@whu.edu.cn

Recommended Citation

Qi-hao LI, Ying-ming WANG, Hua-long MA, Li XIAO, Gong-wei WANG, Jun-tao LU, Lin ZHUANG. A Model for the Anodic Carbonization of Alkaline Polymer Electrolyte Fuel Cells[J]. *Journal of Electrochemistry*, 2020 , 26(5): 731-739.
DOI: 10.13208/j.electrochem.200650
Available at: https://jelectrochem.xmu.edu.cn/journal/vol26/iss5/7

DOI: 10.13208/j.electrochem.200650 **Article ID**:1006-3471(2020)05-0731-09
Cite this: *J. Electrochem*. **2020**, *26*(5): 731-739 **Http**://electrochem.xmu.edu.cn

A Model for the Anodic Carbonization of Alkaline Polymer Electrolyte Fuel Cells

LI Qi-hao, WANG Ying-ming, MA Hua-long, XIAO Li, WANG Gong-wei, LU Jun-tao*, ZHUANG Lin*

(*College of Chemistry and Molecular Sciences, Hubei Key Lab of Electrochemical Power Sources, Wuhan University, Wuhan* 430072, *China*)

Abstract: The alkaline polymer electrolyte fuel cell (APEFC) has made appreciable progress in recent years but is still suffering performance loss during discharge with air as the oxidant. Several theories have been suggested to interpret the loss. However, efforts are still needed to reach a clear quantitative understanding. Based on the major experimental findings in combination with thermodynamics and kinetics of the reactions involved in the anode, this paper presents a model featuring layered carbonization in the anode and relevant grouped equations. The simulation results generated from the latter are compared with experiments, and possible principles to suppress the performance loss are proposed.

Key words: alkaline polymer electrolyte; fuel cell; carbonization; carbon dioxide; hydrogen oxidation reaction

CLC Number: O646 **Document Code:** A

As an integrated part of the sustainable energy system for the future, the fuel cell technology has made great progress in the past decades. There have been several types of fuel cells, among which the proton electrolyte membrane fuel cell (PEMFC) is the most mature today and has started commercial promotion. However, the strong acidic nature of proton electrolyte membranes makes it necessary to depend on Pt based catalysts, of which the high cost and very low natural abundance on the earth have been a major bottle neck for successful commercialization. In order to get rid of the dependence on noble metals, the alkaline polymer electrolyte fuel cell (APEFC) emerged about two decades ago, and has made important progress. In recent years, APEFCs have been able to generate power densities comparable to those of PEMFCs[1-2]. Unfortunately, APEFCs are still suffering own special problems, among which the carbonization during discharge with air as the oxidant is most serious. Compared with the situation of using synthesized air (CO_2 free), the maximum power density of APEFCs using ambient air is roughly cut to a half. The reduced conductivity of the alkaline membrane was the first recognized reason for the performance loss due to carbonization. But researchers soon have realized that the increase in membrane resistance due to carbonization is not the main cause of performance loss. Inaba and coworkers measured the polarization curves of anode and cathode separately and proved that the performance loss occurred mainly in the anode[3-4]. However, it is not yet fully analyzed how the anodic carbonization can depress the performance so much. For example, no picture has been presented with persuasive reasoning for the carbonization distribution inside the anode, let along any attempts to simulate the polarization curve with carbonization. Besides the anodic carbonization, other possible reasons were also suggested in the literature such as thermodynamic, ohmic and kinetic voltage losses[5-6]. Some researchers highlighted thermody-

Received: 2020-07-05, Revised: 2020-09-25 *Corresponding author, Tel: (86-27)68753833, E-mails: jtlu@whu.edu.cn, lzhuang@whu.edu.cn

namic voltage loss more than the kinetic one[7-8].

In the present work, we focus on the problems related to anodic carbonization. The thermodynamics and kinetics of the major reactions involved in the carbonized anode are to be discussed first, followed by description of the main features of our proposed model for the anodic carbonization. Finally, we try to simulate the anodic polarization curve with carbonization and compare the results with experiments.

1 The Three-Reaction System in the Carbonized Anode

1.1 Thermodynamics

The anodic carbonization involves a rather complicated reaction system, involving CO_3^{2-}, HCO_3^-, CO_2, OH^- and H_2O. However, for the most important working mode of APEFCs, this system may be reasonably simplified. It has been pointed out[9] that the carbonization process of alkali might be roughly divided into two main stages, the first being the coexistence of OH^- and CO_3^{2-} while the second the coexistence of CO_3^{2-} and HCO_3^-. It is well known that the anodic carbonization decreases with increasing the discharge current density for APEFCs[10]. In view of the real application of APEFCs, such as the main power source for electric vehicles, the current density is expected to be around or above 1 A·cm^{-2}, so that we shall focus on the system without HCO_3^-, *i.e*., the carbonization mostly remains at the first stage. In such a system, there are three reactions:

$$H_2 + 2OH^- = 2H_2O + 2e$$

$$E^0_{H/OH} = -0.828 \text{ V (vs. SHE)} \quad (1)$$

$$H_2 + CO_3^{2-} = CO_2 + H_2O + 2e$$

$$E^0_{H/C} = -0.535 \text{ V (vs. SHE)} \quad (2)$$

$$CO_3^{2-} + H_2O = 2OH^- + CO_2$$

$$K \quad (3)$$

The three reactions are not independent to each other. For example, Reaction 3 = Reaction 1 - Reaction 2. The relationships among the three reactions are schematically shown in Fig. 1. Both Reactions 1 and 2 are electrode reactions, which exchange electric charges with the same electrode and, therefore, always share the same electrode potential. On the other hand, the reactants and products in the two

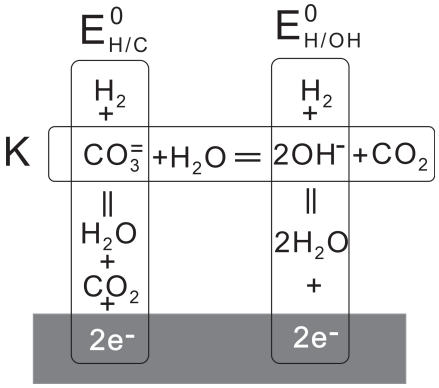

Fig. 1 Schematic presentation of the three reactions coexisting in the carbonized anode of APEFCs.

electrode reactions all play roles in Reaction 3.

The equilibrium constant K for Reaction 3

$$K = \frac{[OH^-]^2[CO_2]}{[CO_3^{2-}][H_2O]}$$

can be calculated based on thermodynamic data or, equivalently, the standard electrode potentials $E^0_{H/OH}$ and $E^0_{H/C}$. The calculated results are given in Fig. 2, which shows K increasing with temperature. When other components are kept unchanged in concentration, the partial pressure of CO_2 also increases with temperature.

With a known K, one can now go further to calculate the anionic concentrations in carbonized alkaline polymer electrolyte (APE) in equilibrium with a given CO_2 pressure. To be kept in mind in the calculation is that the concentrations of the coexisting anions are not independent to each other: $[OH^-] + 2[CO_3^{2-}] = [N]$, where [N] is the concentration

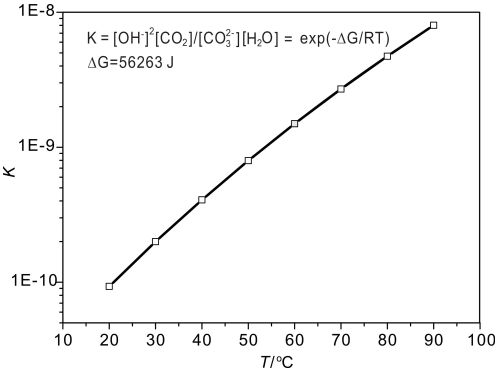

Fig. 2 Calculated equilibrium constant K for Reaction 3.

of the fixed cations in the polymer determined by the ionic exchange capacity (IEC). In the calculation, it was assumed that [N] = 1 mol·L^{-1} and water activity [H_2O] = 1. The results are shown in Fig. 3 where the degree of carbonization appears rather impressive. Raising temperature can depress carbonization, but the influence is limited. For example, even at 80 ℃ with only 1 ppm CO_2, the [OH^-] is below 0.05 mol·L^{-1} compared to the original 1 mol·L^{-1}; while with 200 ppm CO_2, [OH^-] is reduced to only 2.4 mmol·L^{-1}.

With the relevant concentrations known, the equilibrium potentials for the electrode reactions 1 and 2 can be readily calculated. The calculated equilibrium potentials for the two electrode reactions turns out to be identical. This is not a surprise. In fact, it is the manifestation of the equilibrium of the whole system shown in Fig. 1. It is very important to note that the two electrode reactions have identical equilibrium potential. Because it means that at any given potentials the two electrode reactions are experiencing identical overpotential too, which is crucial for understanding the mechanism of the whole electrode process. On the other hand, we are also interested in the value of the equilibrium potential shift caused by carbonization, which is shown in Fig. 4, where the shift is defined as $\Delta E = E_{eq} + 0.828$ V. The potential shift appears to be rather large and very sensitive to CO_2. In air with 400 ppm CO_2, the shift is 0.18 V, and even with only 0.1 ppm CO_2 the potential shift is still notable, 0.06 V.

The large electrode potential shift, at a glance, would lead one to think about the relevant loss of the electrical motive force (EMF) of an APEFC operated in air. However, the carbonization was found, in fact, to cause little change in the open circuit voltage, as proved experimentally by Inaba and coworkers [3-4]. This is because both the oxygen cathode and hydrogen anode have the same dependence on pH that is influenced by carbonization.

1.2 Kinetics

Among the two electrode reactions, Reaction 1 is the "normal" HOR in comparison with Reaction 2. Although the kinetics of HOR on Pt in alkaline media has been found much slower than in acids, it is still fast enough to support APEFCs performing comparably with PEMFCs, provided that sufficient catalyst loading is applied. The serious performance loss of APEFCs working with air leads one to think about the possible decrease in the exchange current i^0 for HOR. There might be two possible factors influencing i^0, *i.e.*, pH change and possible poisoning effects of carbonate anions. Yushan Yan and coworkers investigated the pH dependence of i^0 for HOR and HER (hydrogen evolution reaction) on Pt-group metals in the range pH 0 ~ 13[11]. They found that i^0 decreases with increasing pH in general but levels off in the high pH region (about pH > 11). We measured the HOR with a Pt rotating disk electrode (RDE) in KOH and

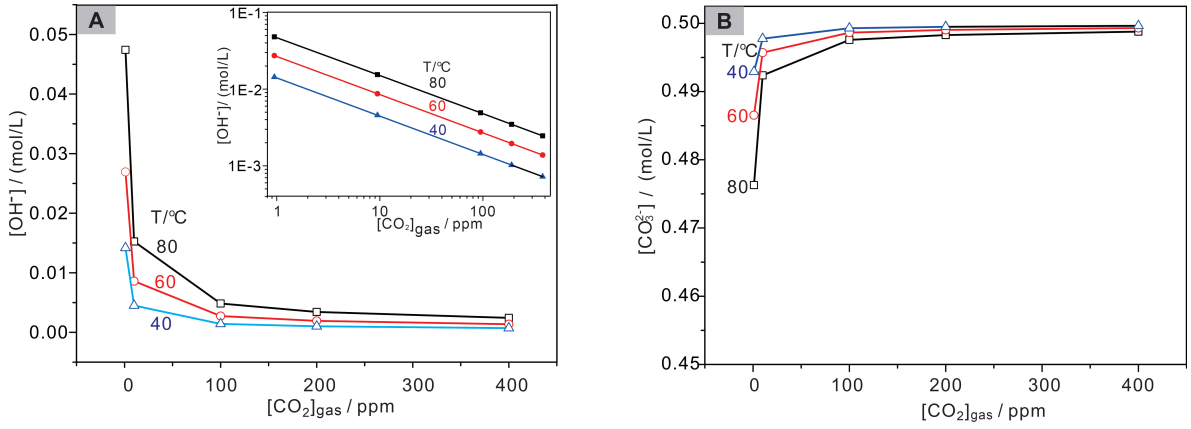

Fig. 3 Calculated concentrations of OH^- (A) and CO_3^{2-} (B) in alkaline polymer electrolyte in equilibrium, with varying CO_2 concentration in the gas phase.

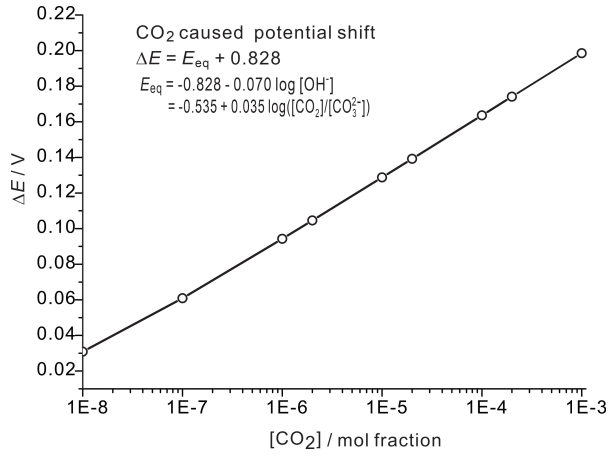

Fig. 4 Calculated potential shift of the anode in equilibrium, with varying CO_2 mole fraction at 80 ℃.

K_2CO_3 mixed solutions (Fig. 5). At a glance, carbonization seems to moderately reduce the HOR activity. However, the apparent differences between the curves were in fact caused by the difference in hydrogen solubility and/or diffusivity. In order to check the real change of HOR activity, the i^0 values for the curves in Fig. 5 were calculated using the equation developed in our previous paper[12], which took into account the changes of both the effective equilibrium potential and the effective i^0 due to surface concentration change of the dissolved hydrogen. On the other hand, the same paper pointed out that i^0 is proportional to the square root of the hydrogen concentration in the solution. Therefore, in order to compare the real HOR activities, the i^0 values were further processed

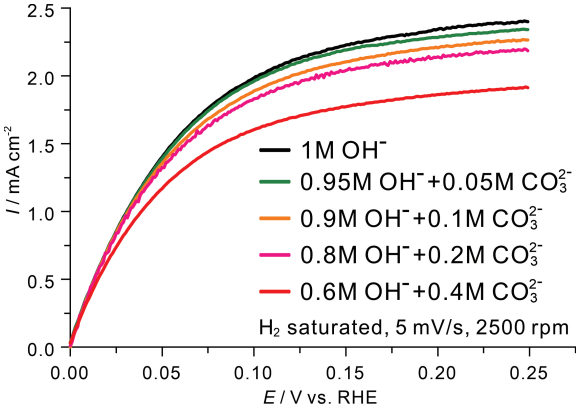

Fig. 5 HOR polarization curves with Pt-RDE in KOH-K_2CO_3 solutions

by normalizing for the square root of the limiting current, i_d. The results showed that within the solution compositions in Fig. 5, the HOR activity is almost kept unchanged. For example, in 1 mol·L^{-1} KOH and 0.6 mol·L^{-1} KOH + 0.4 mol·L^{-1} K_2CO_3, the thus calculated apparent exchange currents were 0.76 and 0.67 mA with the ratios of $i^0/i_d^{1/2}$ being 0.49 and 0.48, respectively. This result is in accordance with the pH dependence trend revealed by Yan and coworkers, *i.e.*, the pH dependence of HOR in strong alkaline media is negligible; more importantly, it proves that carbonate ions do not have appreciable poisoning effects on the HOR. Based on the above discussion, we believe that the observed performance loss is not caused by the i^0 decrease for Reaction 1. As pointed out in a review[9], the slow down effect on HOR in the anode of APEFCs should stem from the depletion of OH^-. Unlike the situation in RDE measurements where there is plenty supply of OH^- from the bulk of solution, in the nano-sized pores of the carbonized anode, OH^- will be quickly depleted on discharge.

After OH^- depletion, the anodic discharge has to depend mainly on the HOR of CO_3^{2-}. The latter can proceed in two paths in principle, *i.e.*, the direct path Reaction 2 and the indirect path Reaction 3 followed by Reaction 1. To the best knowledge of the authors, the kinetics of either Reactions 2 or Reaction 3 has not been well investigated and no relevant data are available at present. For the time being, what we can judge is only that both Reaction 2 and Reaction 3 should be much slower than Reaction 1.

2 Proposed Model for Anodic Carbonization

In the literature, the distribution of carbonization inside the anode is scarcely mentioned. For example, in a review on the APEFC carbonization[9], a curve for the degree of carbonization was drawn in the membrane but the rectangular areas representing the anode and cathode were both left blank. Inaba and coworkers[3-4] drew a curve across both the membrane and the anode but gave neither detailed description nor reasoning. In the text below, a detailed model is presented, featuring layered distribution of carboniza-

tion degree in the anode thickness.

2.1 Carbonization Distribution in the Thickness of the Anode

Based on two major facts, the anodic carbonization must be distributed in a layered mode in the thickness of the electrode: the outer side being deeply carbonized and the inner side slightly carbonized.

It is well known that CO_2 is continuously released to the anodic exhaust when an APEFC is fed with air in the cathode. According to Reaction 3, it is clear that CO_2 would have been absorbed before releasing if the equilibrium had not been established. In other words, the equilibrium of Reaction 3 is the prerequisite for the anodic release of CO_2. Therefore, the outer side of anode must be deeply carbonized with the anionic composition conforming to those shown in Fig. 3.

It is also well known that the anionic reactants needed for HOR in the anode, namely, OH^- and CO_3^{2-}, are coming from the cathode and transported to anode by migration though the membrane. According to the principle of material balance, the anionic composition that enters the anode must be equal to that produced at the cathode. Obviously, this anionic composition is dependent on the discharge current density and the CO_2 concentration in the oxidant gas. When air is used and the current densities are in the range for prospective major applications, around or above 1 $A \cdot cm^{-2}$, CO_3^{2-} accounts for only about 1% or less of the charge carries in the membrane. At meaningful low current densities, such as tens $mA \cdot cm^{-2}$, the CO_3^{2-} migration number may reach 0.1 ~ 0.2, which is still much lower than that in the situation of deep carbonization, in which the CO_3^{2-} migration number is close to unity. Therefore, one can be sure that the inner side of the anode is only slightly carbonized.

The above discussions have settled the two boundary conditions for the carbonization distribution across the anode thickness: outer side deeply carbonized and inner side slightly carbonized. Between the two extremes, there must be a transforming region. The curve of carbonization as a function of the anode thickness is determined by a number of factors, including migration, diffusion and the local reactions these anions participate. For the time being, the authors are making no attempts to deal with this problem

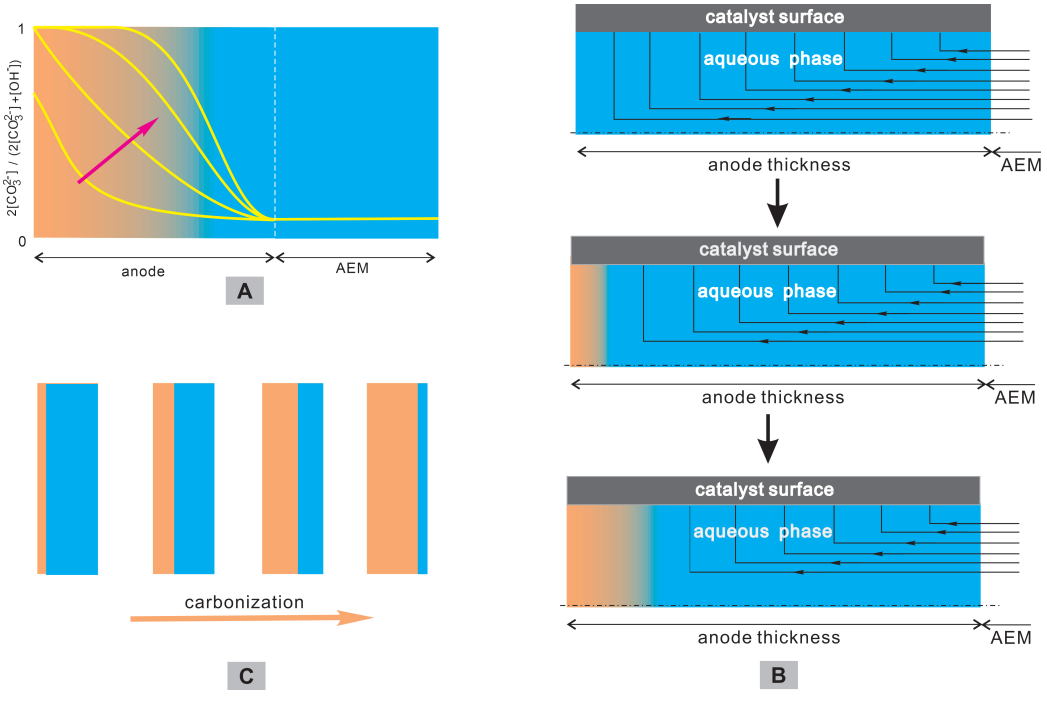

Fig. 6 Proposed model for anodic carbonization. (A) Schematic presentation of the carbonization distribution in electrode thickness; (B) development of anodic carbonization; (C) a simplified presentation of carbonization distribution.

mathematically. In Fig. 6, drawings are given to illustrate qualitatively the proposed model. The carbonization degrees are marked by colors, orange for deep carbonization while blue for slight carbonization. The curves in Fig. 6A are drawn by intuition only. In some discussions it would be helpful to simplify the picture to Fig. 6C, where the anode is simply divided into two layers, one deeply carbonized to the equilibrium of Reaction 3 and the other without carbonization at all.

2.2 Development of Anodic Carbonization

Fig. 6B explains how carbonization develops in the anode. The main rectangle in the figure represents the cross section of the upper half of a shortened liquid pore penetrating the anode thickness. The dot-dashed line on the bottom of the rectangle is the axis of the pore and the lower half of the pore is not shown for symmetric reason. The lines with arrows are the anionic flows and the gray area on the top represents the catalyst. On discharge, CO_3^{2-} ions start to form at the cathode and move through the alkaline electrolyte membrane (AEM) as a part of the charge carriers toward the anode along the arrow lines. Because of the low reactivity of CO_3^{2-} for HOR, it has a low probability to be consumed during migration. As a result, the majority of CO_3^{2-} survives the long journey and reaches the outer side of anode to pile up there till the establishment of equilibrium for Reaction 3. The high concentration of CO_3^{2-} thus formed at the outer side causes diffusion backward which balances with migration to establish a steady state, in which the flowrate of CO_3^{2-} entering the anode inner surface is equal to the flowrate of CO_2 releasing from the anode outer surface.

2.3 Anodic CO_2 Release

For steady discharge using air as an oxidant, anodic CO_2 release is necessary for APEFCs. The CO_2 released from the anode is produced by the HOR of CO_3^{2-} inside the anode. As mentioned above, this reaction may proceed directly or indirectly, but the net reaction is always Reaction 2. Obviously, the major place for this HOR to take place is the deeply carbonized region, *i.e.*, the outer side of the anode. It is

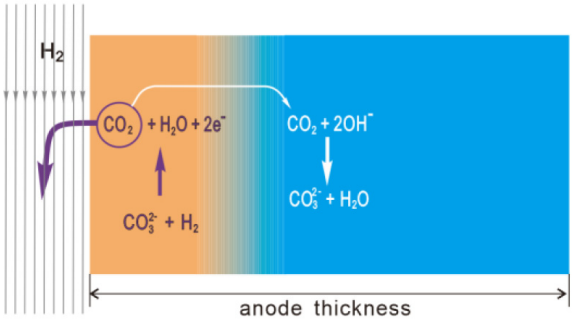

Fig. 7 Production in and release from the outer side of the anode for CO_2.

interesting to note that the location of CO_2 major production happens to be the most favorable place for CO_2 to escape to the exhaust. Of cause, there may be a small part of the thus-formed CO_2 diffuses through the gaseous network of the porous anode to the region of low carbonization and reacts with OH^- there to produce CO_3^{2-} again. In this series of processes, the net change is $2OH^-$ being consumed for HOR and a CO_3^{2-} moved to low carbonization region, no contribution to the CO_2 anodic release.

2.4 The Mathematical Model

Based on the simplified picture of anodic carbonization (Fig. 6C), and the foregoing description of anodic CO_2 production and release, two grouped equations can be established to relate all the relevant variables. Denote the total discharge current and the current produced by CO_3^{2-} participated HOR as I and I_{CO_3}, the deeply carbonized thickness fraction x_{CO_3} and the electrode overpotential η, respectively, two grouped equations can be written:

$$I_{CO_3} = x_{CO_3} f_{CO_3}(\eta) \tag{4}$$

$$I - I_{CO_3} = (1 - x_{CO_3}) f_{OH}(\eta) \tag{5}$$

where $f_{CO_3}(\eta)$ and $f_{OH}(\eta)$ are the current functions for the two HORs. Equations 4 and 5 describe the reaction rates of Reactions 1 and 2, respectively. As pointed in previous section, these two HORs have identical equilibrium potential, therefore they have the same overpotential for any given electrode potentials. If the functions $f_{CO_3}(\eta)$ and $f_{OH}(\eta)$ are known, η and x_{CO_3} can be solved for any set (I, I_{CO_3}) and, in turn,

the η versus I curve can be reconstructed. Unfortunately, $f_{CO_3}(\eta)$ and $f_{OH}(\eta)$ are not yet available for the time being. In the next we shall try to simulate the experimental η versus I curve on some assumptions for simplicity.

According to our experiments, the HOR in alkaline media on Pt is roughly linear in the potential region of interest (data to be reported elsewhere). Therefore, the current function $f_{OH}(\eta)$ was taken as linear, such as $f_{OH}(\eta) = 20\eta$, which means for η = 0.1 V, I = 2 A (or A·cm^{-2}). It must be emphasized that the data set (I, I_{CO_3}) cannot be taken arbitrarily. The I versus I_{CO_3} relationship is in fact determined by the cathode. Unless the CO_2 absorption mechanism in the cathode is well understood so that (I, I_{CO_3}) can be theoretically calculated, we have to depend on the experiment values, such as shown in Fig. 8B. Theoretically, a given cathode can be matched with any anode to form an APEFC and, therefore, once a series of (I, I_{CO_3}) data has been obtained from a real cathode experimentally, it can be used in simulation for any anodes. On other hand, however, the anodic polarization curve η vs. I changes with the cathodic behavior when the APEFC is working on CO_2 containing oxidant gas. Therefore, in order to simulate the polarization curve in a real APEFC, it is necessary to use the true (I, I_{CO_3}) data obtained experimentally in the same APEFC.

Fig. 8 presents both the experimental data and simulation results for an APEFC. Fig. 8A is typical in our laboratory for APEFCs discharging with different oxidant gases. In comparison with that obtained in synthetic air, the discharge curve in air shows additional voltage losses, which increase with discharge current quickly at the beginning but gradually be-

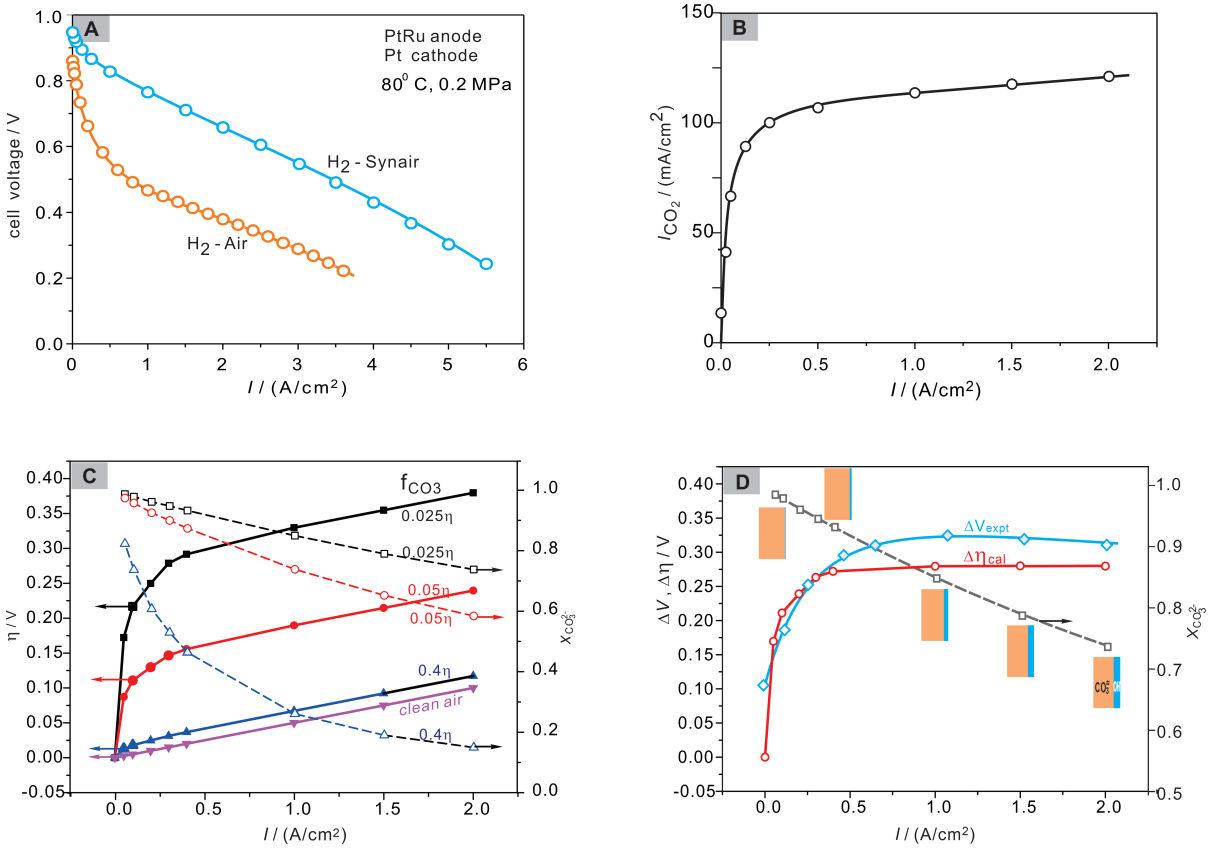

Fig. 8 Simulation of anodic polarization curve. (A) Experimental current-voltage curves of an APEFC; (B) measured I_{CO_3} vs. I; (C) calculated anodic polarization curves (solid lines) and carbonization distributions (dashed lines) for different $f_{CO_3}(\eta)$; (D) comparison with experimental results.

come roughly constant. Fig. 8B is the experimental I_{CO_3} versus I relationship based on the measured rate of anodic CO_2 release. In Fig. 8C, the straight line marked "clean air" is the calculated anodic polarization curve without CO_2 effects and was obtained by simply using $I = f_{OH}(\eta) = 20\eta$. All other solid curves in Fig. 8C are for cases with CO_2 effects, the current function $f_{OH}(\eta)$ for all these curves remained to be the same, namely 20η while $f_{CO_3}(\eta)$ differed as marked on the curves. The vertical distance between the solid curve and the straight line "clean air" represents the additional overpotential due to CO_2 effects. Fig. 8C indicates that the calculated additional anodic overpotential depends on $f_{CO_3}(\eta)$, which reflects the reactivity of CO_3^{2-} for HOR (Reaction 2): the higher the reactivity, the smaller the additional overpotential. For example, when $f_{CO_3}(\eta)$ changes from 0.025η to 0.4η representing CO_3^{2-} activity increasing toward HOR by a factor of 16, the maximum vertical distance decreases from 0.28 V to below 20 mV. In the large current region, the additional overpotential is approximately inversely proportional to $f_{CO_3}(\eta)$. The simulated curve using $f_{CO_3}(\eta)=0.025\eta$ shows the best match with the experimental, as shown in Fig. 8D. The calculated additional anodic overpotential $\Delta\eta$ and the experimentally measured additional cell voltage loss ΔV show similar dependence on the discharge current I, indicative of the cell performance loss being mainly caused by anodic carbonization. Also shown in Fig.s 8C and D are the calculated carbonized thickness fractions, x_{CO_3}, which decreases with increasing CO_3^{2-} activity and increasing discharge current, as expected.

The current function $f_{CO_3}(\eta)$ may not be always linear. For example, unlike our data shown in Fig. 8A, where the V vs. I curves with and without CO_2 are approximately parallel to each other in high current region, it was also reported in the literature that the two curves gradually met again in high current region[3-4]. In the latter case, the current function $f_{CO_3}(\eta)$ must increase with η faster than linear. Relevant modeling works remain to be done in the future.

3 Summary

A model featuring layered anodic carbonization is proposed for alkaline polymer electrolyte fuel cells working with air as oxidant. This model is supported by favorable comparison of simulation results with experimental data. According to this model, the key to suppress the harmful effects of CO_2 on APEFC performance is to enhance the reactivity of CO_3^{2-} toward the hydrogen oxidation reaction in the carbonized region inside the anode. This model remains to be further checked by additional independent experiments, while searching for catalysts to enhance CO_3^{2-} reactivity presents a new scientific challenge. Relevant works are under way in our laboratory.

Acknowledgements

This work was financially supported by the National Natural Science Foundation of China (No. 21991154).

References:

[1] Li Q H, Peng H Q, Wang Y M, et al. The comparability of Pt to Pt-Ru in catalyzing the hydrogen oxidation reaction for alkaline polymer electrolyte fuel cells operated at 80 ℃ [J]. Angewandte Chemie International Edition, 2019, 58 (5), 1442-1446.

[2] Huang G, Mandal M, Peng Xet al. Composite poly(norbornene) anion conducting membranes for achieving durability, water management and high power(3.4 W/cm^2) in hydrogen/oxygen alkaline fuel cells[J]. Journal of The Electrochemical Society, 2019, 166(10): F637-F644.

[3] Matsui Y, Saito M, Tasaka A, et al. Influence of carbon dioxide on the performance of anion-exchange membrane fuel cells[J]. ECS Transactions, 2010, 25(13): 105-110.

[4] Inaba M, Matsui Y, Saito M, et al. Effects of carbon dioxide on the performance of anion-exchange membrane fuel cells[J]. Electrochemistry, 2011, 79(5): 322-325.

[5] Zheng Y W, Omasta T J, Peng X, et al. Quantifying and elucidating the effect of CO_2 on the thermodynamics, kinetics and charge transport of AEMFCs[J]. Energy & Environmental Science, 2019, 12(9): 2806-2819.

[6] Zheng Y W, Huang G, Wang L Q, et al. Effect of reacting gas flowrates and hydration on the carbonation of anion exchange membrane fuel cells in the presence of CO_2[J]. Journal of Power Sources, 2020, 467: 228350.

[7] John S S, Atkinson R W, Roy A, et al. The effect of carbonate and pH on hydrogen oxidation and oxygen reduction

on Pt-based electrocatalysts in alkaline media[J]. Journal of The Electrochemical Society, 2016, 163(3): F291-F295.

[8] Vega J A, Chartier C, Smith S, et al. Effect of carbonate on oxygen reduction, hydrogen oxidation and anion exchange membrane chemical stability[J]. ECS Transactions, 2010, 33(1): 1735-1749.

[9] Ziv N, Mustain W E, Dekel D R. The effect of ambient carbon dioxide on anion-exchange membrane fuel cells[J]. ChemSusChem, 2018, 11(7): 1136-1150.

[10] Krewer U, Weinzierl C, Ziv N, et al. Impact of carbonation processes in anion exchange membrane fuel cells[J]. Electrochimica Acta, 2018, 263: 433-446.

[11] Zheng J, Sheng W C, Zhuang Z B, et al. Universal dependence of hydrogen oxidation and evolution reaction activity of platinum-group metals on pH and hydrogen binding energy[J]. Science Advances, 2016, 2(3): e1501602.

[12] Tang D P, Lu J T, Zhuang L, et al. Calculations of the exchange current density for hydrogen electrode reactions: A short review and a new equation[J]. Journal of Electroanalytical Chemistry, 2010, 644(2): 144-149.

碱性膜燃料电池阳极碳酸化模型研究

李启浩,王英明,马华隆,肖　丽,王功伟,陆君涛*,庄　林*

(武汉大学化学与分子科学学院,湖北省化学电源重点实验室,湖北 武汉 430072)

摘要: 碱性聚电解质燃料电池(APEFC)近年来取得了可观的进展,但是在使用空气作为氧化剂工作时仍然面临着性能损失. 文献中已有多个理论试图解释性能损失的来源, 但是缺乏定量化的分析. 本文根据实验发现和热力学及阳极反应的动力学分析,提出了分层的阳极碳酸化模型和方程组.模型的定量化模拟结果进一步和实验结果进行验证,提出了电池性能损失的可能原因.

关键词: 碱性聚电解质;燃料电池;碳酸化;二氧化碳;氢氧化